

An Experimental Study on A Trapezoidal Pendulum Wave Energy Converter in Regular Waves*

WANG Dong-jiao (王冬姣), QIU Shou-qiang (邱守强)¹ and YE Jia-wei (叶家玮)

*School of Civil Engineering and Transportation, South China University of Technology,
Guangzhou 510640, China*

(Received 19 May 2013; received revised form 26 August 2014; accepted 28 October 2014)

ABSTRACT

Experimental studies were conducted on a trapezoidal pendulum wave energy converter in regular waves. To obtain the incident wave height, the analytical method (AM) was used to separate the incident and reflected waves propagating in a wave flume by analysing wave records measured at two locations. The response amplitude operator (RAO), primary conversion efficiency and the total conversion efficiency of the wave energy converter were studied; furthermore, the power take-off damping coefficients corresponding to the load resistances in the experiment were also obtained. The findings demonstrate that the natural period for a pendulum wave energy converter is relatively large. A lower load resistance gives rise to a larger damping coefficient. The model shows relatively higher wave energy conversion efficiency in the range of 1.0–1.2 s for the incident wave period. The maximum primary conversion efficiency achieved was 55.5%, and the maximum overall conversion efficiency was 39.4%.

Key words: *pendulum wave energy converter; load resistance; wave energy conversion efficiency*

1. Introduction

The consumption of energy has arisen sharply with the rapid development of our society and the economy. New energy resources have become a public-relation hit due to the depletion of conventional energy resources, deterioration of the environment and so on. Much effort has been devoted to develop wave energy converters to extract energy from the sea waves; therefore, the exploitation of ocean energy has been given great importance by many marine countries in the world. As one of the most abundant renewable energy forms, wave energy presents one of the most effective ways to solve the energy crisis. Wave power generation is one of the most common ways to utilise wave energy. There are generally three conversion stages for wave energy to be converted to electricity. The first stage is the so-called power take-off apparatus that is designed to extract energy from ocean waves, the secondary stage is to convert energy from the apparatus in the first stage to mechanical energy or hydraulic energy, and the last stage is electricity output by converting the generally rotating mechanical energy or hydraulic energy forms stored in the secondary stage into electrical energy. Presently, several methods can be proposed to classify wave energy devices according to working location, working principle, and the size of the device (Falcão, 2010; López *et al.*, 2013). There are mainly three types of technologically mature wave energy converters according to their working principle. These are the

* The research was financially supported by the Special Fund for Marine Renewable Energy of the Ministry of Finance of China (Grant No. GD2010ZC02).

¹ Corresponding author. E-mail: qiushouqiang@163.com

oscillating water column (OWC) type (Masuda, 1979; Whittaker *et al.*, 1993; Boccotti, 2007), the oscillating bodies type (Budal *et al.*, 1982; Salter, 1974; Pizer *et al.*, 2005; Whittaker *et al.*, 2007) and the overtopping type (Mehlum, 1986; Kofoed *et al.*, 2006; Margheritini *et al.*, 2007; Vicinanza and Frigaard, 2008). Of these, the mini-watt OWC type has been successfully used on navigation buoys and towers (Masuda, 1971).

The pendulum wave energy converter studied in the present paper works in a pitching mode, which moves forward and backward against a bottom shaft to extract wave energy and is usually classified into the oscillating body type. Early theoretical models and analytical results have been developed by Mei (1976), Newman (1977) and Evans (1985). Generally there are two types of pendulum wave energy converters studied presently in the world, which are the gravitational pendulum and buoyant pendulum types, respectively, according to the installation position of the rotating shaft. A series of studies on the former type which utilises a part of the coastal structures have been performed by the group of faculties of Muroran Institute of Technology in Japan since 1978 (Kondo *et al.*, 1984). Experimental studies were conducted at the initial stage and subsequently a field test plant was constructed at Muroran Port. The system had an oscillating pendulum around the horizontal axis perpendicular to it, and it transmitted the power of the pendulum to that of oil pressure through a reciprocating cylinder connected to the pendulum at the top. The pendulum had a weight of 2.5 tons, a width of 2.0 m and a height of 3.5 m (Kondo *et al.*, 1984). In addition to the former types, a number of concepts of the latter type have been proposed including the Oyster (Whittaker *et al.*, 2007), Waveroller (<http://www.aw-energy.com>), and bioWAVE (<http://www.biopowersystems.com>). Aquamarine Power's 315 kW Oyster 1 prototype was deployed at the European Marine Energy Centre of Orkney in August 2009 and later Oyster 2, which was installed in the summer of 2011 was designed as an improvement on Oyster 1 (Whittaker *et al.*, 2007). The Oyster was basically a wave-powered pump driving water at high pressure through pipelines to a high-head hydroelectric plant onshore. The pendulum-type wave energy converters can be deployed at the near-shore and intermediate-water-depth oceans (Caska and Finnigan, 2008; Flocard and Finnigan, 2010). In China, studies on this type of wave energy converter are in its infancy. Qiu *et al.* (2011a, 2011b), Zhao *et al.* (2013), Wang *et al.* (2014a, 2014b) and Zhang *et al.* (2014) have conducted their initial work in this area. However, all of their studies were in the laboratory and theoretical stage. A pendulum wave energy converter was experimentally studied in the present paper at a model scale. A generator is connected to the shaft by adding a matched gearing-up or hydraulic booster between them and then load resistances can be applied to the generator for electricity output.

In the experimental test of the model, incident waves, generated by the wave maker, travel along the wave flume and then interact with the pendulum flap. However, waves were combined in the wave flume as the sum of the waves that were reflected by the model flap and those radiated by the flap itself. In reality, the incident waves cannot be recorded directly. This leads to the necessary separation of the composite waves and has always been a common problem that takes place when carrying out model tests in the wave flume. The incident wave height separated from the composite waves has to be considered to simulate the real state of the sea. It is common to analyse the wave elevations logged by two or three wave gauges located in front of the model in the wave flume to properly find the actual

amplitude of the incident waves. Separation methods are mainly the two-point method (Goda and Suzuki, 1976), three-point method (Mansard and Funke, 1980), transfer function method (Zhu, 1999), analysis method (AM) (Wang *et al.*, 2003). The AM method was chosen in the present study to separate the composite waves. Similar studies on a cylinder-type pendulum wave energy converter were carried out by the authors. The readers can refer to Qiu *et al.* (2013) for the results and more information.

2. Experimental Rigs

Experiments were carried out in a wave flume, which is 32 m×1.0 m×1.5 m in length, width and height, respectively. There is a push-plate-type wave maker at one end of the flume and a breakwater at the other end. The pendulum wave energy converter model tested in the present paper is a bottom-hinged type with its rotating shaft fixed on an underwater base. Two wave gauges were deployed at a distance of 0.3 m between the wave maker and the model in the wave flume to monitor the water elevation that was to be separated to obtain the incident wave height. The flap pitches forward and backward under the action of the incident waves. A second rotating shaft which is coupled to the underwater shaft by a stainless steel wire is mounted above the water surface to support some sensors. A generator is also coupled to the top shaft by a gearing-up booster for electricity output. Moreover, two tension sensors are attached in the middle of the stainless steel wire to record the tension of the wire when the flap is acted upon by the excited waves. The excited wave torque against the bottom shaft of the flap can then be obtained by multiplying the tension by the lever arm. Meanwhile, the pitching angle of the flap can also be received by an angular encoder deployed on one end of the top shaft. The layout of the experimental setup is illustrated in Fig. 1.

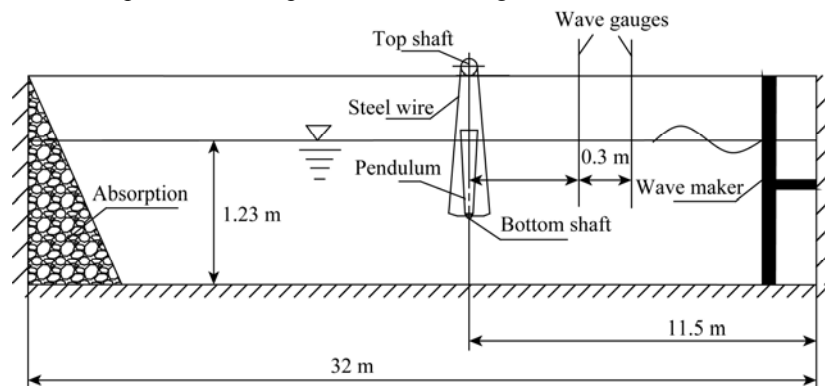


Fig. 1. Layout of experimental setup in the wave flume.

The model with a height of 710 mm, width of 630 mm and thickness at the bottom and top of 70 mm and 145 mm, respectively, is shown in Fig. 2 and the physical model of the flap is shown in Figs. 3 and 4. Borders with a width of 35 mm and thickness of 1 mm were attached on both sides of the pendulum flap, and two strengthening skeletons were located symmetrically at a distance of 210 mm from the outer side. The bottom shaft was fixed on the top of an underwater

rail which spans the width of the flume and at a height of 590 mm from the bottom of the wave channel. The flap moves forward and backward to absorb wave energy excited by the waves with a moment of inertia against the bottom shaft of $2.38 \text{ kg}\cdot\text{m}^2$.

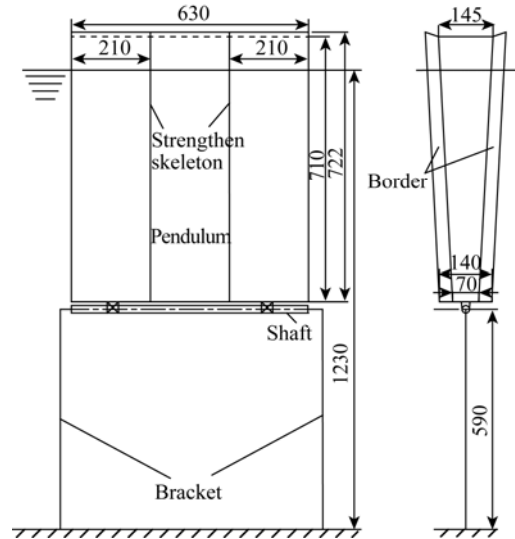


Fig. 2. Experimental model of the pendulum wave energy converter.



Fig. 3. The flap model (side view).

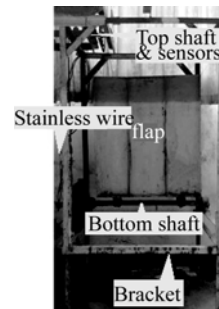


Fig. 4. The flap model and the bracket (front view).

3. Motion Response and Conversion Efficiency

The wave energy converter is connected to an electrical system which will affect the motion of the converter and can absorb the wave energy. The motion equation of a fixed pendulum wave energy converter connected to the electrical system can be modelled by using a single degree of freedom system in the time domain as:

$$[I + J(\infty)]\ddot{\theta}(t) + \int_{-\infty}^t K(t-\tau)\dot{\theta}(\tau)d\tau + B_N|\dot{\theta}(t)|\dot{\theta}(t) + M_p(t) + C\theta(t) = M_w(t), \quad (1)$$

where I is the moment of inertia for the device against the bottom rotating shaft, $J(\infty)$ is the infinite frequency-dependent added-mass moment of inertia, $K(t)$ is the retardation function (impulse

response), B_N is the nonlinear viscous damping coefficient and C is the restoring moment coefficient. The angle $\theta(t)$ is the pitch angle of the device and $M_W(t)$ is the wave-exciting moment. $M_p(t)$ is the moment due to the applied power take-off damping and may be expressed as:

$$M_p(t) = B_p \dot{\theta}(t). \quad (2)$$

where B_p is the power take-off damping coefficient which was applied by load resistances coupled to the generator in the case of our tests.

Experiments were conducted in regular waves, and the incident wave height H was obtained by separation of the composite waves that were recorded by the wave gauges. We make the pitching angular of the flap positive when moving forward as opposed to its equilibrium position in still water and negative when moving backward. The response function of motion can then be described as follows, with θ_{\max} defined as the positive maximum and θ_{\min} the negative minimum, respectively.

$$RAO = \frac{\theta_{\max} - \theta_{\min}}{H}. \quad (3)$$

For the intermediate water depth wave conditions studied, the incident wave power (P_{in}) with a wave height H in the model scale can be written as:

$$P_{in} = \frac{\rho g \omega H^2 L}{16k} \left[1 + \frac{2kd}{\sinh(2kd)} \right], \quad (4)$$

where

$$\omega = \sqrt{gk \tanh(kd)}, \quad (5)$$

L is the width of the pendulum flap, d is the water depth, k is the wave number, ρ is the water density, g is the acceleration due to gravity, and ω is the wave frequency.

The power output of the flap can then be obtained as follows:

$$P(t) = M_p(t) \frac{d\theta}{dt}. \quad (6)$$

In the case of our test, the average power output of the pendulum flap (P_m) in a wave cycle can be expressed as:

$$P_m = \frac{1}{T} \int_0^T M_p(t) \frac{d\theta}{dt} dt. \quad (7)$$

According to Eq. (2), Eq. (7) can also be written as:

$$P_m = \frac{1}{T} \int_0^T B_p \left(\frac{d\theta}{dt} \right)^2 dt, \quad (8)$$

In consideration of Eqs. (7) and (8), the power take-off damping coefficient (B_p) corresponding to the load resistances in the experiments can be easily obtained as follows:

$$B_p = \frac{P_m}{\frac{1}{T} \int_0^T \left(\frac{d\theta}{dt} \right)^2 dt}. \quad (9)$$

The instantaneous electricity output (P_{out}) can be achieved by applying load resistances on the

generator and can be expressed as the following equation,

$$P_{\text{out}}(t) = \frac{U(t)^2}{R}, \quad (10)$$

where R is the load resistance and $U(t)$ is the voltage across the load resistance. Then, the average electricity output can be obtained and expressed as \bar{P}_{out} . The primary energy conversion efficiency is written as:

$$\eta_1 = \frac{P_m}{P_{\text{in}}}. \quad (11)$$

And the final energy conversion efficiency is given by

$$\eta = \frac{\bar{P}_{\text{out}}}{P_{\text{in}}}. \quad (12)$$

4. Analysis of Results

The AM method (Wang *et al.*, 2003) was chosen to separate the composite waves recorded from the experiments in the wave flume. We make $\zeta_I(x, t) = \text{Re}[\eta_I(x, t)]$ and $\zeta_R(x, t) = \text{Re}[\eta_R(x, t)]$ be the wave surface elevation of the incident wave propagating towards the device and reflected wave propagating away from the device, respectively, in which $\eta_I(x, t)$ and $\eta_R(x, t)$ are given by

$$\eta_I(x, t) = A_I \exp[i(\omega t - kx + \theta_I)]; \quad (13)$$

$$\eta_R(x, t) = A_R \exp[i(\omega t + kx + \theta_R)], \quad (14)$$

where A_I and A_R are the incident and the reflected wave amplitudes, respectively.

The composite wave elevation at position x_1 and $x_2 = x_1 + \Delta x$ are $\zeta(x_1, t) = \text{Re}[\eta(x_1, t)]$ and $\zeta(x_2, t) = \text{Re}[\eta(x_2, t)]$, in which $\eta(x_1, t)$ and $\eta(x_2, t)$ are

$$\eta(x_1, t) = \eta_I(x_1, t) + \eta_R(x_1, t); \quad (15)$$

$$\eta(x_2, t) = \eta_I(x_1, t) \exp(-ik\Delta x) + \eta_R(x_1, t) \exp(ik\Delta x). \quad (16)$$

The incident wave train can be obtained from Eqs. (15) and (16) as:

$$\eta_I(x_1, t) = \frac{\exp(ik\Delta x)\eta(x_1, t) - \eta(x_2, t)}{2i \sin(k\Delta x)}. \quad (17)$$

In real situations, however, we have only the real parts of the composite waves as measured data, so the Hilbert transform is introduced to obtain the imaginary parts of $\eta(x_1, t)$ and $\eta(x_2, t)$. From the separated incident waves, the wave height H of the incident wave can be easily obtained.

Experimental and numerical results on the response amplitude operator (*RAO*) of the pendulum wave energy converter under the undamped condition as defined above are shown in Fig. 5, where T denotes the wave period and H is the wave height in regular waves. The reader can refer to Wang *et al.* (2014b) for the numerical method. It is demonstrated that the natural period of the pendulum flap is fairly large and that *RAO* is sensitive to the wave height H near the resonant region as mentioned by Wang *et al.* (2014b). Furthermore, it is indicated that the nonlinear viscous damping plays an important

role in the dynamic response of the wave energy converter especially in the vicinity of the natural period.

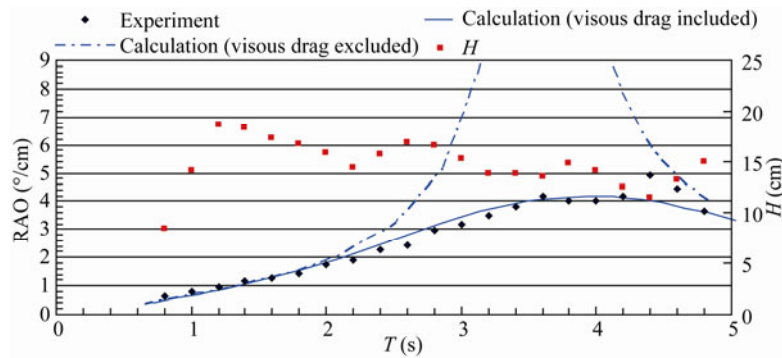


Fig. 5. Incident wave height and RAOs for an undamped converter (viscous drag term was included for comparison).

Different damping coefficients can be achieved by setting variable load resistances, and five different load resistances, $R=8.5 \Omega$, 11Ω , 13Ω , 15Ω , and 18Ω were applied in the experiments. Interrelation analyses of the load resistances, wave periods and wave energy conversion efficiency were carried out. Fig. 6 displays the variation of the damping coefficient corresponding to those of the load resistances. It is clear from the results that a smaller load resistance can accordingly result in a larger damping coefficient. The damping tends to increase gently with the increase of wave period while the load resistance maintains constant. The pendulum flap responds forward in the downstream direction and backward in the upstream direction periodically, but in the case of our tests, the load resistances were applied only when the flap moved forward, that is the flap activated as a single-acting mode. RAOs for different load resistances are performed in Fig. 7. It is shown that a large damping coefficient results in a small response as expected.

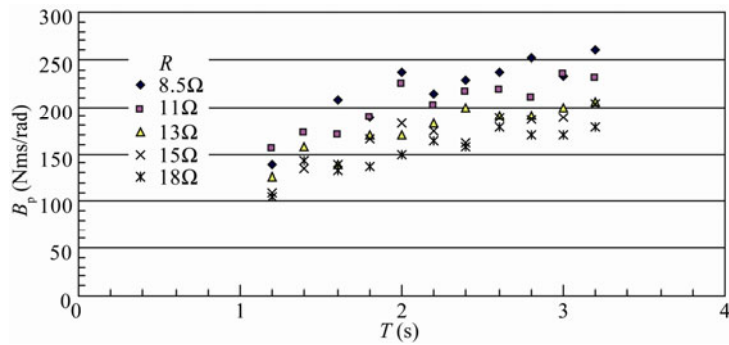


Fig. 6. Damping functions for different load resistances.

Fig. 8 illustrates the primary energy conversion efficiency of the pendulum wave energy converter for different load resistances, and the overall conversion efficiency for the converter subjected to regular waves is displayed in Fig. 9. It is evident from Fig. 8 that a maximum primary conversion efficiency of 55.5% can be achieved with a wave period of $T=1.2$ s and the load resistance $R=11 \Omega$. The best performance is observed in Fig. 9 where the overall conversion efficiency can reach a

maximum of 39.4% at a wave period of $T=1.0$ s and the load resistance of $R=13 \Omega$. It is also shown in Fig. 9 that an optimal overall energy conversion efficiency can be obtained over the range of wave period $T=1.0-1.2$ s, and it is unfavourable to take into consideration of applying the power take-off when the wave period is smaller than 1.0 s, where a sharp decline can be observed. For the case of load resistance $R=13 \Omega$, the mean output power P_m/H^2 of the flap and the incident wave power P_{in}/H^2 are shown in Fig. 10. It is shown that, under the same conditions of wave height, the incident wave power obtained from Eq. (4) increases rapidly with the increase of wave period, but the changes of the mean power output P_m/H^2 are not obvious compared with the incident wave power P_{in}/H^2 . Despite the larger response motion of the flap that occurs at wave period $T=3$ s, the wave energy conversion efficiency is not high because the incident wave power is bigger.

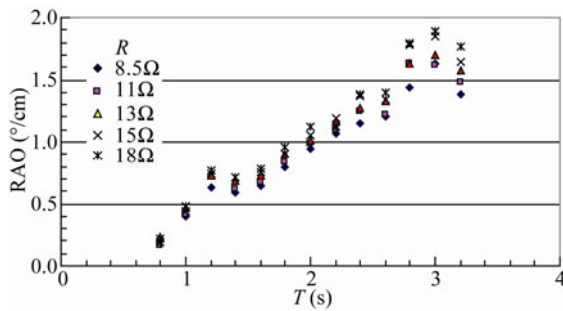


Fig. 7. RAOs for the pendulum flap under different load resistances.

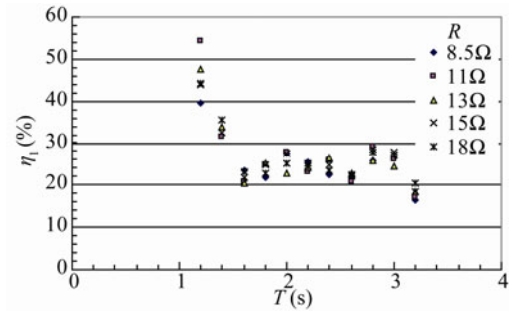


Fig. 8. Primary conversion efficiency for the converter subjected to regular waves.

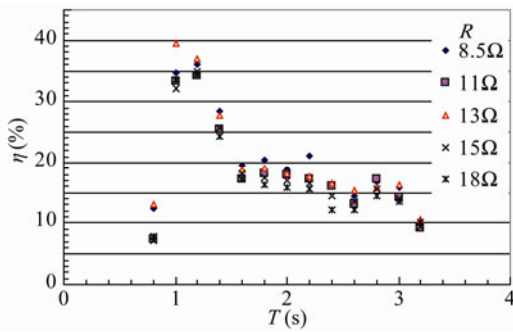


Fig. 9. Overall conversion efficiency for the converter subjected to regular waves.

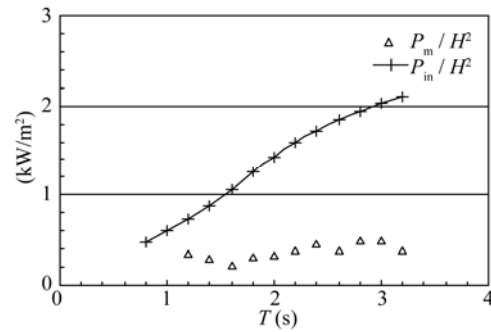


Fig. 10. Incident wave power and the mean power output of the flap under load resistance $R=13 \Omega$.

5. Conclusions

It can be concluded from the experiments conducted above that

- (1) The pendulum wave energy converter has a large natural period in the case of our tests.
- (2) An relatively higher overall energy conversion efficiency can be obtained over the range of $T=1.0-1.2$ s for the cases of our tests, where the optimal primary wave energy conversion efficiency reaches 55.5% maximally and the overall conversion efficiency can reach 39.4%. It is unfavourable to

take into consideration of applying the power take-off when the wave period is smaller than 1.0 s, where a sharp decline can be observed in the experiments.

(3) A small dynamic response is observed as expected for the pendulum wave energy converter with a small load resistance, where the corresponding damping coefficient is large.

(4) The final conversion efficiency was low near the natural period despite a larger pitching response occurred; the reason was that the incident wave energy was large too.

References

- Boccotti, P., 2007. Caisson breakwaters embodying an OWC with a small opening, Part I: Theory, *Ocean Eng.*, **34**(5): 806–919.
- Budal, K., Falnes, J., Iversen, L. C., Lillebekken, P. M., Oltedal, G., Hals, T. and Høy, A. S., 1982. The Norwegian wave-power buoy project, *Proceedings of 2nd International Symposium on Wave Energy Utilization*, Trondheim, Norway, 323–344.
- Caska, A. J. and Finnigan, T. D., 2008. Hydrodynamic characteristics of a cylindrical bottom-pivoted wave energy absorber, *Ocean Eng.*, **35**(1): 6–16.
- Evans, D. V., 1985. The hydrodynamic efficiency of wave energy devices, in: *Hydrodynamics of Ocean Wave Energy Utilisation*, Lisbon, 1–34.
- Falcão, A. F. O., 2010. Wave energy utilization: A review of the technologies, *Renew. Sust. Energ. Rev.*, **14**(3): 899–918.
- Flocard, F. and Finnigan, T. D., 2010. Laboratory experiments on the power capture of pitching vertical cylinders in waves, *Ocean Eng.*, **37**(11-12): 989–997.
- Goda, Y. and Suzuki, Y., 1976. Estimation of incident and reflected waves in random wave experiments, *Proceedings of the 15th Conference on Coastal Engineering*, Honolulu, Hawaii, 828–845.
- Kofoed, J. P., Frigaard, P., Friis-Madsen, E. and Sørensen, H. C., 2006. Prototype testing of the wave energy converter wave dragon, *Renew. Energ.*, **31**(2): 181–189.
- Kondo, H., Watabe, T. and Yano, K., 1984. Wave power extraction at coastal structure by means of moving body in the chamber, *Proceedings of the 19th Conference on Coastal Engineering*, Houston, Texas, 2875–2891.
- López, I., Andreu, J., Ceballos, S., de Alegria, I. M. and Kortabarria, I., 2013. Review of wave energy technologies and the necessary power-equipment, *Renew. Sust. Energ. Rev.*, **27**, 413–434.
- Mansard, E. P. and Funke, E. R., 1980. The measurement of incident and reflected spectra using a least squares method, *Proceedings of the 17th Conference on Coastal Engineering*, Sydney, Australia, 154–172.
- Margheritini, L., Vicinanza, D. and Kofoed, J. P., 2007. Hydraulic characteristics of seawave slot-cone generator pilot plant at Kvitsøy (Norway), *Proceedings of the 7th European Wave Tidal Energy Conference*, Porto, Portugal.
- Masuda, Y., 1971. *Wave-Activated Generator*, Int. Colloq Exposition Oceans, France, Bordeaux.
- Masuda, Y., 1979. Experimental full-scale results of wave power machine Kaimei in 1978, *Proceedings of the 1st Symposium on Wave Energy Utilization*, Gothenburg, Sweden, 349–363.
- Mehlum, E. T., 1986. *Hydrodynamics of Ocean Wave Energy Utilization*, Berlin, Springer, 51–55.
- Mei, C. C., 1976. Power extraction from water waves, *J. Ship Res.*, **20**, 63–66.
- Newman, J. N., 1977. *Marine Hydrodynamics*, Cambridge, MA, MIT Press.
- Pizer, D. J., Retzler, C., Henderson, R. M., Cowieson, F. L., Shaw, M. G., Dickens, B. and Hart, R., 2005. Pelamis WEC—recent advances in the numerical and experimental modeling programme, *Proceedings of the 6th European Wave Tidal Energy Conference*, Glasgow, UK, 373–378.

- Qiu, S. Q., Ye, J. W., Wang, D. J. and Liang, F. L., 2011a. Investigation on the efficiency of a pendulum energy converter in regular waves, *Proceedings of the 21st International Offshore and Polar Engineering Conference*, Maui, Hawaii, USA, 650–654.
- Qiu, S. Q., Ye, J. W., Wang, D. J. and Liang, F. L., 2011b. Capture width study on a pendulum wave energy converter, *Proceedings of 2011 Asia-Pacific Power and Energy Engineering Conference*, Wuhan, China, 1–4.
- Qiu, S. Q., Ye, J. W., Wang, D. J. and Liang, F. L., 2013. Experimental study on a pendulum wave energy converter, *China Ocean Eng.*, **27**(3): 343–352.
- Salter, S. H., 1974. Wave power, *Nature*, **249**, 720–724.
- Wang, D. J., Qiu, S. Q. and Ye, J. W., 2014a. Study on the hydrodynamics of a single-acting pendulum wave energy converter, *Appl. Mech. Mater.*, **518**, 209–214.
- Wang, D. J., Qiu, S. Q. and Ye, J. W., 2014b. Study on hydrodynamics of a trapezoidal pendulum wave energy converter, *Acta Energetica Solaris Sinica*, **35**(4): 589–593. (in Chinese)
- Wang, Y. X., Peng, J. P., Sun, H. Q. and Li, G. W., 2003. Separation of composite waves by an analytical method, *The Ocean Engineering*, **21**(1): 42–46. (in Chinese).
- Whittaker, T., Collier, D., Folley, M., Osterried, M., Henry, A. and Crowley, M., 2007. The development of Oyster – A shallow water surging wave energy device, *Proceedings of the 7th European Wave and Tidal Energy Conference*, Porto, Portugal.
- Whittaker, T., McIlwaine, S. J. and Raghunathan, S., 1993. A review of the Islay shoreline wave power station, *Proceedings of First European Wave Energy Symposium*, 283–286.
- Vicinanza, D. and Frigaard, P., 2008. Wave pressure acting on a seawave slot-cone generator, *Coast. Eng.*, **55**(6): 553–568.
- Zhang, D. H., Li, W., Zhao, H. T., Bao, J. W. and Lin, Y. G., 2014. Design of a hydraulic power take-off system for the wave energy device with an inverse pendulum, *China Ocean Eng.*, **28**(2): 283–292.
- Zhao, H. T., Sun, Z. L., Hao, C. L. and Shen, J. F., 2013. Numerical modeling on hydrodynamic performance of a bottom-hinged flap wave energy converter, *China Ocean Eng.*, **27**(1): 73–86.
- Zhu, S. T., 1999. Separation of regular waves by a transfer function method, *Ocean Eng.*, **26**(12): 1435–1446.